ON THE WATER ENHANCED TURBOFAN CONCEPT: PART B - FLOW PATH AND MASS ASSESSMENT

Jannik Häßy[1], Alexander Görtz[1], Marc Schmelcher[1], Jens Schmeink[1] & Mahmoud El-Soueidan[1]

[1]German Aerospace Center (DLR), Linder Höhe, 51147 Cologne, Germany

Abstract

Aviation is responsible for a growing portion of global greenhouse gas emissions contributing to climate change. The Water-Enhanced Turbofan (WET) is a promising concept for reducing the climate impact of aviation in terms of CO_2 and Non-CO_2 effects. The innovative thermodynamic cycle with a quasi-closed water circuit increases overall efficiency and reduces emissions. However, one challenge is the size and mass of the propulsion system in terms of installation and fuel burn penalties. This work deals with the estimation of the flow path and system mass on conceptual level. A comparison is made between a WET and a conventional geared turbofan architecture to assess the difference in integration space and mass. Compared to a geared turbofan architecture, the model predictions for the WET concept show an increase of only 36 % in engine length and 84 % in bare engine mass. These conceptual design results indicate that the WET concept could be feasible in terms of integration space and system mass. Additionally, the impact of the bypass ratio and overall pressure ratio on dimensions, mass and fuel burn are discussed.

Keywords: Propulsion, Aero Engine, Conceptual Design, Water-Enhanced Turbofan

1. Introduction

Aviation is responsible for a considerable portion of global greenhouse gas emissions contributing to climate change. With proceeding decarbonization in different private and industrial sectors, the portion of aviation is expected to grow continuously if no counter measures are implemented. It is a major challenge to further reduce emissions and the impact of aviation on climate to achieve Europe's ambitious targets [1]. Engine technology plays a major role with respect to emissions, primarily due to the use of kerosene from fossil source. Evolutionary development of conventional engine architectures remains important but will not enable the required leap to address current challenges. Therefore, electric propulsion concepts, fuel cell-based propulsion, drop-in capable Sustainable Aviation Fuels (SAFs) and hydrogen are being researched. However, batteries lack the necessary energy density for long-distance travel. Fuel cell-based propulsion systems do not achieve the high power densities of gas turbines and require an active dissipation of waste heat to the ambience. Synthetic fuel production requires excessive renewable energy as well as infrastructure everywhere around the globe, which is not expected to be available in sufficient quantities in the near future. The use of hydrogen imposes further challenges with respect to storage, safety, component life and aircraft design [2, 3].
One promising idea for reducing the climate impact of aviation is the Water-Enhanced Turbofan (WET) proposed by MTU Aero Engines [4, 5]. The WET concept is a gas turbine-based propulsion concept that can run on hydrogen or sustainable aviation fuels in addition to kerosene from fossil source and can be used for all aircraft classes. The WET utilizes the residual heat from the engine's exhaust gas to increase overall efficiency. In terms of the thermodynamic cycle, a Cheng cycle is implemented, which combines the Joule-Brayton cycle with a Clausius-Rankine cycle in parallel execution [6, 7].
Figure 1 presents the schematic of the WET concept and gives an overview of components and their connections. Superheated water vapor is injected into the combustion chamber, is present during combustion and contributes to power generation in the turbines. Two heat exchangers are used to

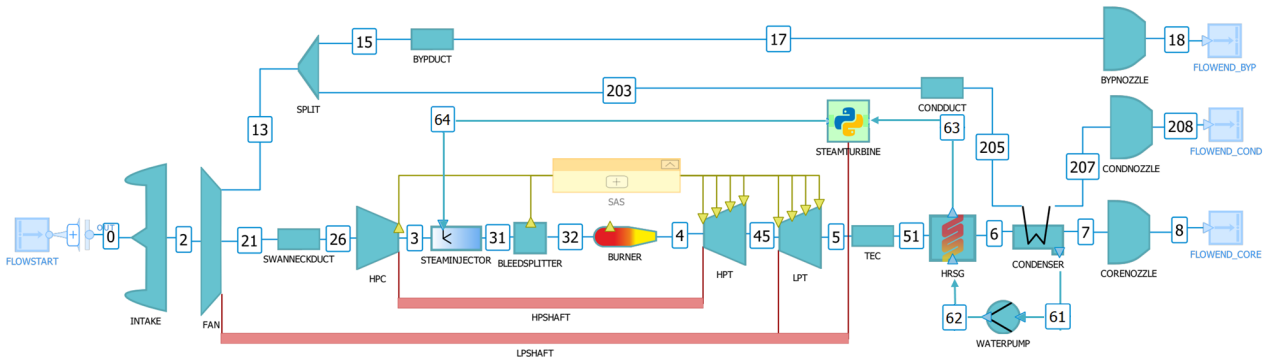

Figure 1 – Schematic of the WET concept.

extract the residual heat from the exhaust gas flow: The first heat exchanger preheats, evaporates and superheats water that is afterwards injected into the combustion chamber by cooling the core exhaust flow. The second heat exchanger uses the bypass flow that is pressurized by the fan to further cool the exhaust gas flow and to condense the contained water. The water is then recovered from the exhaust flow in liquid form before the flow exits the nozzle. The recovered water is pumped to a high-pressure level and is provided to the evaporator. This results in a quasi-closed water circuit. Water that cannot be recovered from the flow and therefore exits the system is compensated by the water that is produced during combustion. As an optional extension, a small steam turbine can be integrated to support the low-pressure shaft. Overall, the thermal efficiency and power density of the engine are increased, allowing higher bypass ratios to be realized with the same fan diameter compared to conventional turbofan architectures [4]. This leads to a decrease in fuel consumption and carbon dioxide (CO_2) emission. Furthermore, the WET has the potential to reduce the non-CO_2 effects that contribute to global warming: First, the injection of water lowers the amount of nitrogen oxides produced during combustion. Second, the WET concept may reduce contrail formation [8]. However, there are still numerous challenges that require investigation.
One challenge is the size and mass of the propulsion system. A heavy and large propulsion system is more difficult to install and leads to fuel burn penalties. Especially, the heat exchangers add system mass and require space for integration. The smaller core engine for the WET concept partly compensates these penalties. This work deals with the estimation of the flow path and system mass for WET on conceptual level. A comparison is made with a conventional turbofan architecture to assess the difference in integration space and mass. The following research questions are addressed.

Research Questions:

1. What are the flow path dimensions for a WET compared to a conventional turbofan architecture?
2. How does the bare engine mass and its breakdown differ for a conventional turbofan architecture and the WET concept?
3. How do the flow path and bare engine mass change with design parameters of the WET? What are the thermodynamic cycle parameters for minimum bare engine mass?

This work (Part B) is complementary to the paper “ON THE WATER ENHANCED TURBOFAN CONCEPT: Part A - Thermodynamics and Overall Engine Design”. Part A focuses on the thermodynamic cycle analysis and presents a method to assess design changes on overall system level with respect to mission fuel burn. Thermodynamic cycle data from part A is the basis for the flow path and mass investigations presented herein. The methods developed here are provided for Part A to estimate overall system performance including penalties related to dimensions and mass. In this paper, the variation of the bypass ratio (BPR) and overall pressure ratio (OPR) is presented with focus on WET dimensions and mass. Further design studies for the WET concept are presented in part A.

2. Methodology

The herein presented studies are conducted by means of the virtual propulsion framework Gas Turbine Laboratory (GTlab). GTlab is developed at the Institute of Propulsion Technology of the German Aerospace Center and provides various modules for multidisciplinary design and analysis of aero engines at different levels of detail [9, 10, 11]. For this paper, relevant modules are extended to model the WET concept.

2.1 Thermodynamic Cycle

The performance program DLRp2 is utilized for thermodynamic cycle analysis of the WET concept, which is described in part A of this work (see [12]). The obtained thermodynamic data for the operating conditions cruise and maximum take-off is the basis for estimating engine geometry, turbomachinery efficiencies and mass. The thermodynamic model is coupled within an iterative workflow with the models described in the following.

2.2 Geometrical Model

The implemented flow path model of the WET is shown in figure 2. The WET consists of a turbomachinery assembly and a heat exchanger assembly. The turbomachinery assembly comprises turbo components and required structural components: fan, swanneck duct, high-pressure compressor (HPC), combustor, high-pressure turbine (HPT), low-pressure turbine (LPT), turbine exhaust case (TEC), gearbox, shafts, frames and required accessories. The heat exchanger assembly consists of the inlet case, core plug, evaporator, cover plate, intermediate duct, condenser, bypass cover plates and engine plug. To close the water-circuit, the WET concept implements further components that are neglected here since their design and model development is ongoing: A steam turbine expands the superheated steam and supports the low-pressure shaft. The water recovery unit extracts the condensed water from the exhaust flow downstream of the condenser. The exhaust gas nozzle guides the core flow to the ambience. However, it is expected that these not modeled components neither are main drivers for overall engine dimensions nor for engine mass.

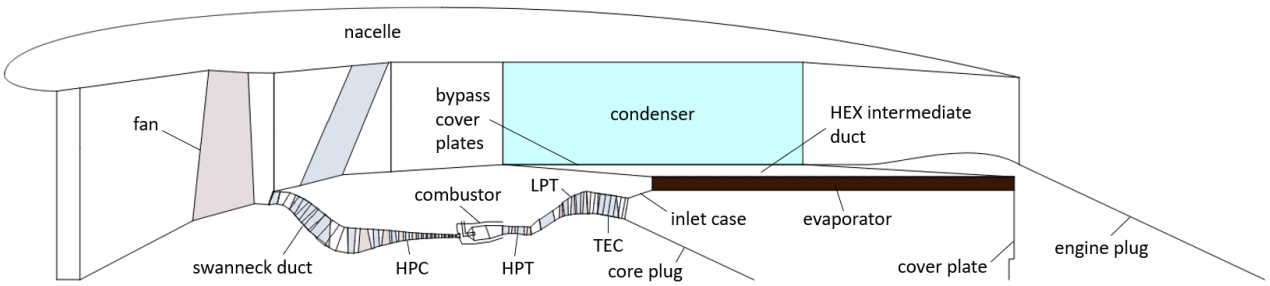

Figure 2 – Geometrical model of the WET.

2.2.1 Turbomachninery Assembly

A conceptual design method for flow path sizing is used to estimate the geometry of the turbomachinery assembly based on thermodynamic parameters and a geometrical knowledge-base [13]. The required non-dimensional parameters, e.g. hub-to-tip ratios, blade aspect ratios and Mach numbers, are taken from a geared turbofan model that serves as reference. Additionally, the following assumptions are introduced:

- **Fan:** A single rotor fan is driven by the low-pressure shaft via a gearbox. The rotational speed of the fan is set by matching a target value for the reduced circumferential velocity at the rotor tip, which is modeled in dependence on the fan pressure ratio according to Grieb [14]. The fan and low-pressure shaft speed define the gear ratio.
- **Swanneck duct:** The length of the swanneck duct depends on the radius difference between the fan's core outlet guide vane and the inlet of the HPC.

- **HPC:** The stage count of the HPC is selected to do not exceed an average stage loading of $\psi = \Delta h/U_m^2 \leq 0.37$. One limiting parameter for estimating the high-pressure shaft speed is a maximum meanline circumferential velocity at the inlet of $U_{m,in} = 420\,m/s$.
- **Combustor:** The system for water injection is assumed to be integrated into the combustor without increasing the combustor length.
- **HPT:** To provide enough power for compression and ensure feasible stage expansion ratios, a HPT with two stages is assumed.
- **LPT:** The stage count of the fast-turning LPT is selected to achieve an average stage loading of $\psi = \Delta h/U_m^2 \leq 1.8$ but three stages are set as a minimum. The maximum allowable meanline circumferential velocity at the outlet is $U_{m,out} = 400\,m/s$ and is considered for estimating the rotational speed of the low-pressure shaft.

2.2.2 Heat Exchanger Assembly

Figure 3 depicts a 3D-view of the geometrical WET model to visualize the flow through the heat exchanger assembly. The exhaust gas, which is highly-loaded with water, exits the core engine at the TEC and flows radially outwards through the tube-bundle type evaporator (red). Inside the tubes, the water is preheated, evaporated and superheated following multiple parallel paths and implementing a cross-counterflow arrangement. Then, the cooled exhaust flow enters the intermediate duct, which connects the evaporator and condenser. The plate-fin type, cross-flow condenser (green) consists of several segments that are integrated into the bypass channel at equally spaced angular positions. Coming from the intermediate duct, the exhaust gas is further cooled by flowing through the condenser segments from the hub to the tip of the bypass channel. On the other side of the condenser plates, bypass air is used to absorb the transferred heat. Only a portion of the bypass air flows through the condenser segments and to achieve an acceptable level of pressure losses for this air, the Mach number has to be reduced from $M =$ 0.45-0.55 to a significantly lower level. The corresponding diffusion device is currently still under investigation and not modeled here. At the exit of the condenser, most of the water of the cooled exhaust flow is liquid. The liquid water is extracted from the flow in the water recovery unit, which is probably integrated into the nacelle but not modeled here.

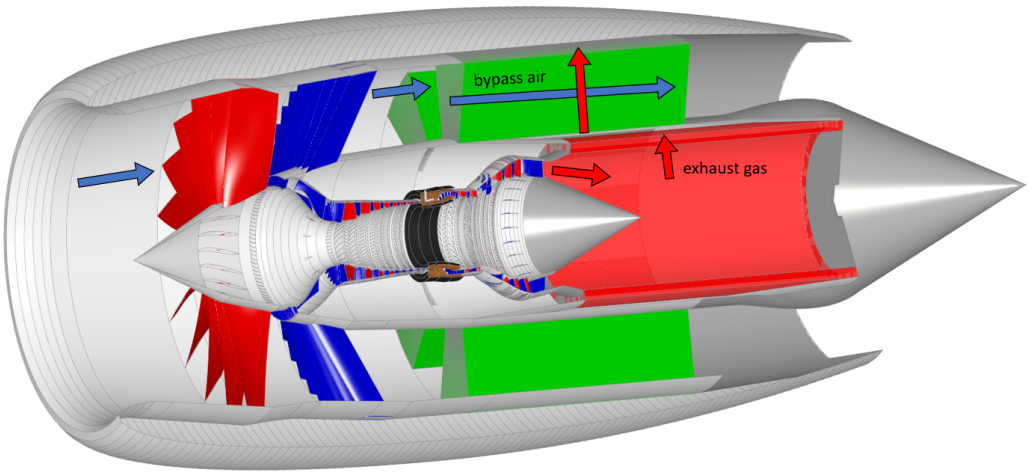

Figure 3 – 3D-view of geometrical WET model.

In order to estimate the dimensions of the heat exchangers, the required transfer area A_{trans} is calculated according to equation 1.

$$Q = U\,A_{trans}\,\Delta T_{log} \tag{1}$$

The transferred heat Q and the logarithmic temperature difference ΔT_{log} between the fluids results from the thermodynamic analysis. The thermodynamic model calculates the temperature profiles for both fluids using multiple segments (see figure 4).

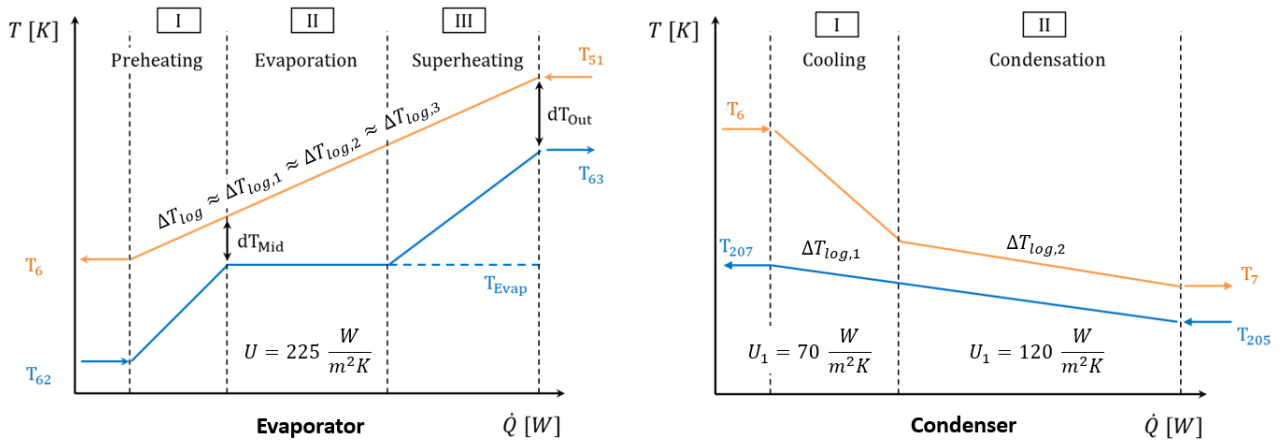

Figure 4 – Temperature profiles for heat exchangers.

The temperature profile for the evaporator was validated by means of a more detailed analysis using the tool PreHEAT [15]. The overall heat transfer coefficient U accounts for convection on both fluid sides and conduction in the wall as well as for the efficiency of fins, if applicable.
Figure 5 shows the geometrical parameterization for the evaporator and the condenser. The evaporator is build using a densely packed tube matrix. The tubes have a small diameter d and wall thickness t and are arranged with the spacing distances s_1, s_2 and s_3. The exhaust gas flows through the matrix (fluid 1) and the water inside the tubes (fluid 2). For the condenser, parallel plates with the thickness t_p are arranged with spacing distances s_1 and s_2. Both sides are equipped with fins of thickness t_f under the angle α_f to increase the available heat transfer area. Heat is transferred from the exhaust gas (fluid 1) to the bypass air (fluid 2). Representative values for the geometrical parameters presented in figure 5 are selected and maintained constant for this work.

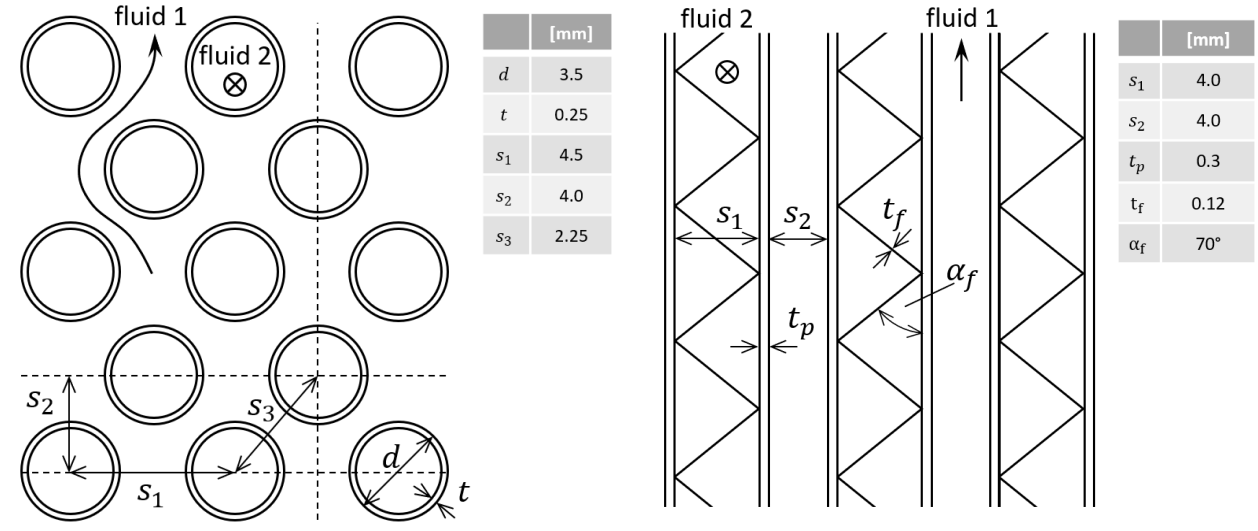

	[mm]
d	3.5
t	0.25
s_1	4.5
s_2	4.0
s_3	2.25

	[mm]
s_1	4.0
s_2	4.0
t_p	0.3
t_f	0.12
α_f	70°

(a) Evaporator (b) Condenser

Figure 5 – Geometrical parameterization of the heat exchangers.

For cruise conditions, overall heat transfer coefficients are assumed for the evaporator with U_{evap} = 225 W/m^2/K and for the condenser with $U_{cond,1}$ = 70 W/m^2/K and $U_{cond,2}$ = 120 W/m^2/K. The overall heat transfer coefficient for the evaporator is derived from a detailed analysis with the tool PreHEAT [15] for a similar set of boundary conditions. The values for the condenser are rather generic assumptions taking into consideration that both fluids are mostly gaseous and the fins have an efficiency < 1. For a given set of geometrical parameters of the heat exchangers, the overall heat transfer coefficient U mainly depends on the Reynolds numbers of the fluids. Maintaining similar inlet conditions, velocity

levels and therefore Reynolds numbers, the assumption of constant overall heat transfer coefficients at cruise is justifiable for comparing different thermodynamic cycles at conceptual level.

$$A_{trans}/V_{evap} = f(d, s_1, s_2, s_3, r_{in}, N_p) \tag{2}$$

$$A_{trans}/V_{cond} = f(t, s_1, s_2, t_f, \alpha_f) \tag{3}$$

The available heat transfer area per volume A/V depends on the geometrical parameters of the heat exchangers (see equations 2 and 3). The parameter r_{in} is the inlet radius of the evaporator and N_p is the number of passenges, i.e. the number of tubes in radial direction. For the assumed geometrical parameters in this work, the transfer area per volume is A/V = 612 m^2/m^3 for the evaporator and A/V = 912 m^2/m^3 for the condenser. The required value of A_{trans}, which is calculated with equation 1, leads in combination with A/V to the heat exchanger volume V. The overall dimensions of the heat exchangers and other components of the heat exchanger assembly are then calculated as follows:

- **Evaporator:** The inlet radius of the evaporator r_{in} scales with the tip radius at the outlet of the core. The inlet frontal area of the evaporator A_{in} is calculated by specifying a representative Mach number for the exhaust flow and therefore, maintaining a similar velocity level for all designs. The axial length of the evaporator follows from the area and radius at the inlet. The evaporator thickness, i.e. number of passages, is calculated based on the total volume V. The pressure loss of the exhaust gas is scaled with the evaporator thickness (see part A [12]).
- **Condenser:** The inlet radius of the condenser depends on the outlet radius of the evaporator and an assumed channel height for the intermediate duct. The outlet radius of the condenser is the same as the tip radius of the fan's outlet guide vane to ensure the installation of the nacelle. Specifying both radii yields the plate height (radial direction) of the condenser. The number of condenser segments in the bypass channel is an input and the circumferential extension of each segment depends on the portion of bypass air that is guided through the condenser segments. Then, the length of the condenser (axial direction) follows from the required condenser volume V. The pressure loss of the bypass air is scaled with the condenser length (see part A [12]).
- **Plugs, ducts and covers:** The core plug, inlet case and cover plate of the evaporator encloses the exhaust gas volume and guide the flow through the evaporator. Their dimensions follow from the geometry of the TEC and the evaporator assuming a certain axial length of the inlet case. The height of the intermediate duct in radial direction is specified as share of the radius at the evaporator outlet. The walls of the intermediate duct are straight lines connecting both heat exchangers and no meaningful aerodynamic shape is defined. The intermediate duct is separated from the bypass flow by means of cover plates that fit between the condenser segments in the hub region of the bypass channel. For the core plug and the engine plug an cone angle of 25° is assumed.

2.3 Mass Estimation

The mass of the turbomachinery assembly is estimated by means of a part-based procedure according to [13] considering e.g. rotor blades, stator vanes, disks, casing parts, sealing devices, variable guide vanes, shafts, structural components like frames and accessories. The following assumptions are introduced:

- **Fan:** The hybrid metallic, hollow rotor blades of the fan are made of Aluminium-Lithium alloy (density ρ = 2700 kg/m^3) with titanium sheet leading edges. Aluminium is used for the core outlet guide vanes (density ρ = 2800 kg/m^3). The fan case is made of carbon fiber reinforced plastic CFRP (density ρ = 1600 kg/m^3) and has a thicker wall as well as a ballistic liner in the region of the rotor blades to provide the required containment capability. CRFP is also assumed for the bypass outlet guide vanes. Titanium is used for the fan disk (density ρ = 4650 kg/m^3).

- **HPC:** Titanium alloy (density ρ = 4650 kg/m^3) is used for front stages, i.e. rotors, vanes, casing, disks. All rear stages that face an maximum operating temperature above 680 K are made of Nickel-based alloy (density ρ = 8200 kg/m^3).
- **Combustor:** Cobalt-based alloy is assumed for the combustor, e.g. Haynes 188 (density ρ = 8950 kg/m^3). The system for water injection is assumed to be integrated into the combustor without increasing the combustor mass.
- **HPT:** Rotor blades and stator vanes are manufactured as single crystals, e.g. CMSX-10 (density ρ = 9020 kg/m^3). Disks and casing parts are made of Nickel-based alloy. The maximum allowable blade pull stress at the disk rim is set to 600 MPa and is a potentially limiting parameter for estimating the rotational speed of the high-pressure shaft.
- **LPT:** Nickel-based alloy is used for front stages. At rear stages that face a maximum operating temperature lower than 1000 K, Titanium-Aluminid (density ρ = 3800 kg/m^3) is assumed for rotor blades only. The maximum allowable blade pull stress is set to 460 MPa and is considered as limit for estimating the low-pressure shaft speed.
- **Shafts:** Nickel-based alloy is assumed for shafts and the required shaft thickness is calculated according to [16].
- **Frames:** Frames are structural components that support shaft bearings and transfer forces to the outer engine case. For the WET concept, the fan frame (Titanium alloy) supports both spools at the front engine. At the rear engine, a frame at the inlet guide vane IGV of the LPT supports the high-pressure shaft and the TEC frame supports the low-pressure shaft (both Nickel-based alloy).
- **Accessories:** An empirical correlation for accessory mass is applied that accounts for the secondary air system, oil system, fuel system, accessory gear box and engine control system.

The mass of the heat exchanger assembly is obtained by estimating the material volume for each component and multiplying it with an assumed density. The following assumptions are introduced:

- **Evaporator Parts:** All parts that face the high temperatures at the core outlet are made of Nickel-based alloy: evaporator tubes, core engine plug, inlet case and cover plate. The thickness of the inlet case and cover plate are set to 3 mm and to 2 mm for the engine plug. Additionally, structural components that carry the heavy tube bundles are assumed to add 15 % of the tube mass.
- **Intermediate duct:** The heat exchanger intermediate duct and bypass cover plates are assumed to be made of Titanium alloy with a wall thickness of 1.5 mm.
- **Condenser:** Titanium alloy is also assumed for the plates and fins of the condenser. Additionally, structural components that carry the heavy condenser segments are assumed to add 15 % of the plate and fin mass.
- **Engine plug:** the engine plug is made of CFRP.
- **Not modeled:** The mass for the water pump, steam turbine and water recovery unit as well as valves, actuators and water tubing system are neglected. However, it is assumed that their contribution to engine mass is rather small compared to the heat exchangers.

2.4 Turbomachinery Efficiency

A correlation-based conceptual design method is applied to predict the polytropic efficiency of turbo components η_p based on the flow path and thermodynamic parameters according to [17]. In a superposition approach, efficiency deltas $\Delta\eta_i$ are added to a baseline value $\eta_{p,base}$ (see equation 4).

$$\eta_p = \eta_{p,base} + \Delta\eta_W + \Delta\eta_{RNI} + \Delta\eta_{EIS} + \Delta\eta_{CA} + \Delta\eta_C \tag{4}$$

The single terms account for the following effects:

- **Baseline value $\eta_{p,base}$:** The baseline value is derived from Smith-type design charts for compressors and turbines of the core engine and accounts for the shape of velocity triangles. The 'inlet-outlet-averaged' approach is used here (see [17]). For the fan, a correlation is used where the baseline efficiency depends on the axial inflow Mach number and the fan pressure ratio.
- **Component size ($\Delta\eta_W$):** Below a certain threshold, small turbo components face a loss in efficiency, e.g. due to increased relative tip clearances or manufacturing tolerances. This effect is modeled based on the corrected mass flow at the component's inlet.
- **Reynolds number index ($\Delta\eta_{RNI}$):** The effect of changing operational conditions is accounted for by the Reynolds number index RNI. For example, the fan efficiency decreases with altitude due to lower Reynolds numbers.
- **Technological maturity ($\Delta\eta_{EIS}$):** The level of component technology depends on the year of entry into service (EIS). A component specific efficiency delta is added according to the assumed EIS = 2035.
- **Blade cooling air ($\Delta\eta_{CA}$):** In case of cooled turbines, an increasing amount of cooling air reduces the turbine efficiency.
- **Calibration factor $\Delta\eta_C$:** A calibration factor for each turbo component type is added. This factor was determined by comparing the correlation predictions with reported database values of several engines [17].

2.5 Iterative Process

Figure 6 shows how the different models are coupled within an iterative workflow. For a given set of input parameters and start values, the thermodynamic cycle is calculated (see part A of this work). Based of the resulting data, the flow path of the WET is predicted. Based on the flow path, a simple aerodynamic analysis is conducted for turbomachinery components and their efficiencies are predicted. Based on thermodynamics, the flow path and material properties, the WET mass is estimated. The rotational shaft speeds are set to match a limiting parameter: either a maximum circumferential blade velocity or the maximum allowable blade pull stress at the disk rim. The predicted efficiencies of turbo components are fed back into the thermodynamic model. A fixed point iteration is applied until the change in turbomachinery efficiency is below a certain tolerance.

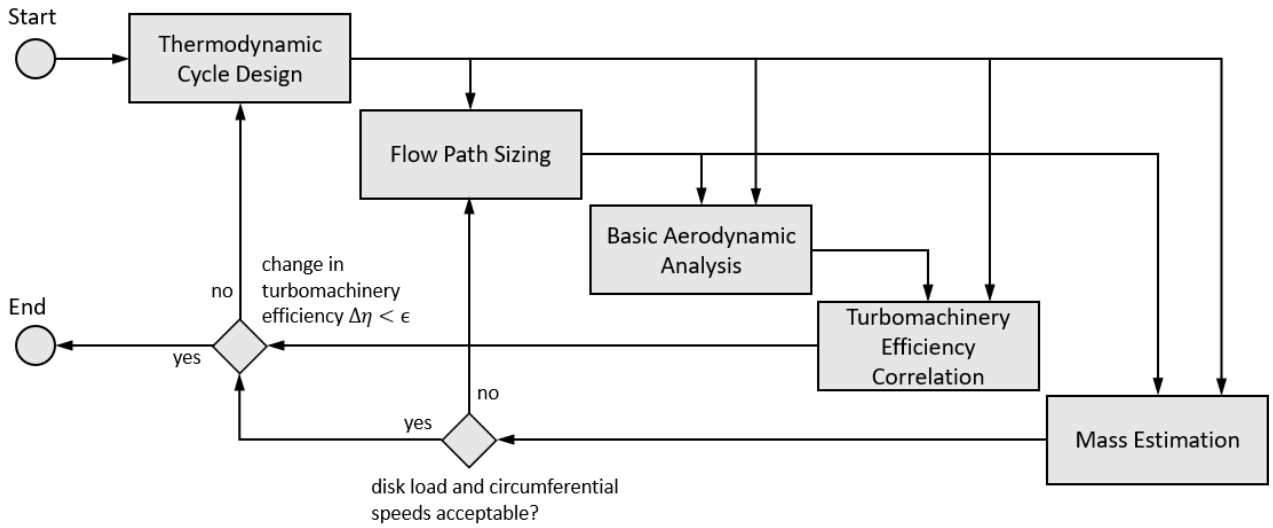

Figure 6 – Workflow for the conceptual design of WET.

3. Comparison of WET and Geared Turbofan

Figure 7 shows a comparison of flow paths for the WET concept and a conventional geard turbofan architecture. Both engines are designed for the same set of requirements and have an equal target fan radius of 1.0287 m. The thermodynamic cycle for each engine architecture is selected to achieve a good overall engine performance in line with technological limits.
The shown flow path of the WET corresponds to a turbine entry temperature of T_4 = 1600 K and an overall pressure ratio of OPR = 30 with a bypass ratio of BPR = 21.8 at cruise operation. A further increase of T_4 or OPR would result in falling below the minimum required blade height of 10.5 mm at the last stage of the HPC. The BPR is determined by matching the prescribed fan radius.
The conventional geared turbofan has an OPR of 44.5, a T_4 of 1700 K and a BPR of 13.3 at cruise operation. The parameters OPR and T_4 are limited by maximum values for the compressor exit temperature at take-off and the stator outlet temperature of the HPT T_{41} at top of climb, respectively. The BPR is determined by matching the prescribed fan radius. With respect to engine geometry, the following observations are made:

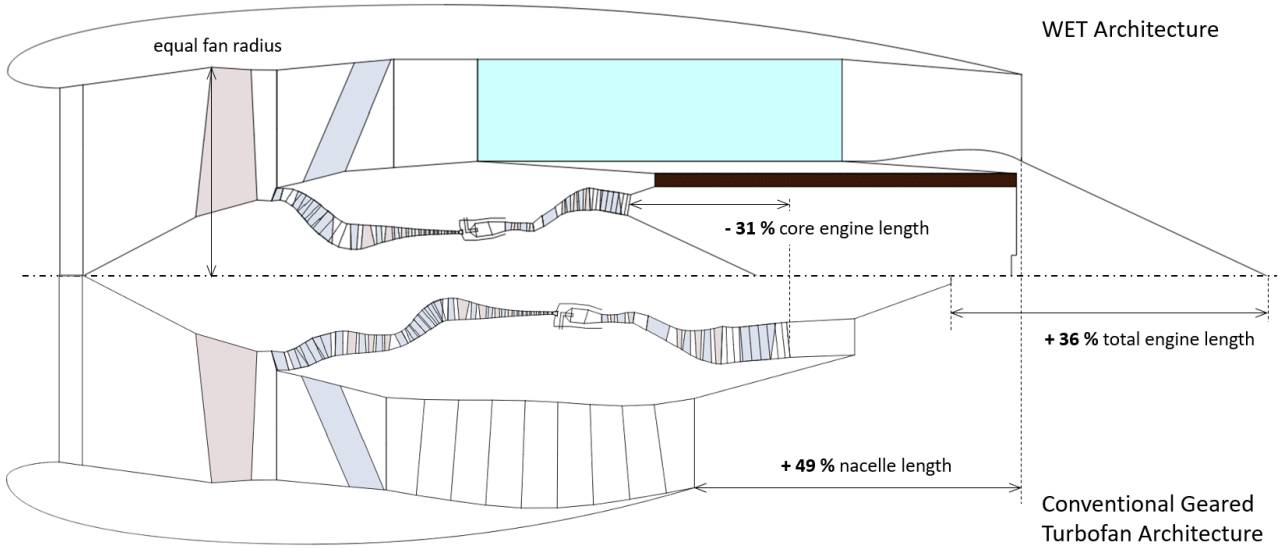

Figure 7 – Comparison of the flow path for the WET concept and a conventional geared turbofan.

- **Core Engine:** The length of the core engine is with -31 % significantly smaller for the WET concept. The specific power of the core is increased due to the water injection and the bypass ratio is higher for the same fan diameter. As a result, blade dimensions shrink even if the OPR is in comparison relatively low. This can be observed especially for the turbine section. Also, the absence of a booster contributes to a smaller core length. The stage count of HPC, HPT and LPT is the same for both architectures.
- **Heat Exchangers:** Even if the core engine is smaller, the WET concept requires large heat exchangers. The length of the evaporator is similar to the length of the core engine. The large condenser in the bypass duct also requires integration space and additional engine length. The axial length of the evaporator and condenser is in the same order of magnitude but the condenser is placed closer to the fan and the intermediate duct has to bridge a large axial off-set to connect both heat exchangers.
- **Overall Engine:** The total engine length of the WET concept increases by 36 % and the nacelle length by 49 % compared to the reference geared turbofan architecture. The increased engine length challenges the integration of the engine under the wing. However, the nacelle radius can be maintained implementing the WET concept. The increased nacelle length and area will lead to additional drag counts and a penalty on overall aircraft level.

The presented numbers give only a first indication: The engine length for the WET concept is higher compared to the reference system but no show stoppers are found in terms of engine size. However, it is emphasized that there is still a large uncertainty in the assumptions made. Additionally, not all options to further reduce engine size are explored for the WET concept.

Architecture	**GTF**			**WET**			**Mass Difference WET - GTF**		
Component	**Total** *[kg]*	**Total** *[lb]*	**Share** *[%]*	**Total** *[kg]*	**Total** *[lb]*	**Share** *[%]*	**abs.** *[kg]*	**abs.** *[lb]*	**rel.** *[%]*
Fan	611	1347	23.1	618	1362	12.6	7	15	1.1
Fan Frame	140	310	5.3	123	272	2.5	-17	-38	-12.2
BOOSTER	105	231	4.0	-	-	-	-	-	-
Intermediate Frame	78	171	2.9	-	-	-	-	-	-
HPC	213	470	8.1	255	562	5.2	42	92	19.5
Combustor	56	124	2.1	60	133	1.2	4	10	7.7
HPT	145	320	5.5	150	330	3.1	4	10	3.1
ITD 1	9	21	0.4	8	19	0.2	-1	-2	-10.8
LPT IGV Frame	20	45	0.8	29	64	0.6	8	18	40.7
LPT	338	746	12.8	335	738	6.9	-3	-7	-1.0
TEC Frame	72	159	2.7	71	156	1.4	-1	-3	-1.8
HP Shaft	7	16	0.3	3	7	0.1	-4	-9	-54.7
LP Shaft	43	95	1.6	23	51	0.5	-20	-44	-46.2
Gearbox	316	697	11.9	335	738	6.9	19	41	5.9
Accessories	494	1090	18.7	357	788	7.3	-137	-302	-27.7
Turbo Engine Assembly	**2650**	**5842**	**100.0**	**2368**	**5220**	**48.5**	**-282**	**-622**	**-10.6**
Core Engine Plug	-	-	-	11	24	0.2	-	-	-
Evaporator Inlet Case	-	-	-	13	29	0.3	-	-	-
Evaporator Cover Plate	-	-	-	20	44	0.4	-	-	-
Evaporator	-	-	-	480	1059	9.8	-	-	-
Evaporator Tubes	-	-	-	*418*	*921*	*8.6*	-	-	-
Evaporator Structure	-	-	-	*63*	*138*	*1.3*	-	-	-
HEX Intermediate Duct	-	-	-	41	91	0.8	-	-	-
Condenser	-	-	-	1903	4195	38.9	-	-	-
Condenser Plates	-	-	-	*761*	*1679*	*15.6*	-	-	-
Condenser Fins	-	-	-	*890*	*1963*	*18.2*	-	-	-
Condenser Structure	-	-	-	*251*	*554*	*5.1*	-	-	-
Bypass Cover Plates	-	-	-	22	49	0.5	-	-	-
Engine Plug	-	-	-	28	61	0.6	-	-	-
Heat Exchanger Assembly	**-**	**-**	**-**	**2519**	**5553**	**51.5**	**-**	**-**	**-**
Bare Engine Mass	**2650**	**5842**	**100.0**	**4886**	**10773**	**100.0**	**2237**	**4931**	**84.4**

Figure 8 – Mass for the WET concept and a conventional geared turbofan.

Figure 8 presents the predicted mass breakdown structure for the geared turbofan and the WET concept. The following observations are made:

- **Fan:** There is only a marginal difference of 1.1 % in fan mass since the fan diameter is the same for both engine architectures. The fan frame is lighter by 12.2 % in case of the WET concept due to a smaller core size and frame radius.
- **Core engine:** The absence of a booster and an intermediate frame reduces the mass for WET but also leads to a lower pressure at the inlet of the HPC. The low air density leads to larger HPC dimensions even if the mass flow is smaller and finally results in a 19.5 % heavier HPC. Also the combustor is larger and heavier due to the lower OPR for the WET concept. The dimensions of the LPT are significantly smaller for the WET concept (see figure 7) and this is reflected in mostly all parts of the LPT. However, the last rotor blade of the geared architecture is made of Titanium-Aluminid and the corresponding disk mass can be reduced. In contrast, the temperature at the last LPT stage for the WET is too high for using the lighter blade material and a heavy disk for rotor blades made of Nickel-based alloy is required. In total, the LPT mass is reduced by only 1 % even if the size of the LPT is significantly smaller for WET. The mass of the low-pressure shaft is lower for WET due to the reduced core length. A large absolute mass reduction of 137 kg comes from engine accessories and is related to the smaller core size.

- **Turbomachinery assembly:** The turbomachinery assembly is 10.6 % lighter for the WET concept comparing with a conventional geared turbofan. The turbomachinery assembly weighs 2650 kg in case of the geared turbofan architecture and 2368 kg in case of the WET architecture. The largest portion of mass reduction is related to the absence of the booster and the intermediate frame as well as less accessory mass. Unfortunately, the uncertainty of the used correlation for accessories is expected to be high. The resulting turbomachinery mass reduction of 10.6 % estimated here is in good agreement with the prediction of 15 % less turbomachinery mass presented by Schmitz et al. [4].
- **Heat exchanger assembly:** The mass of the engine plug, inlet case and cover plate do only marginally contribute to the total mass of the heat exchanger assembly. The evaporator is with a mass of 480 kg significantly lighter than the condenser with 1903 kg. The large number and area of thin condenser plates equipped with fins make up the largest portion of the condenser mass. The intermediate duct and bypass cover plates are predicted with a total mass of 63 kg. This mass is related to the large radius and the axial gap that has to be bridged between the heat exchangers. The engine plug is with 28 kg rather light. The total mass of the heat exchanger assembly is 2519 kg, which is in the same order of magnitude as the turbomachinery assembly mass.
- **Total bare engine:** The predicted total bare engine mass is 2650 kg for the geared turbofan and 4886 kg for the WET concept. In comparison, the WET concept is 84 % heavier. This is related to the mass increase due to the heat exchangers which can not be compensated by mass reductions of the core engine. Especially the condenser significantly contributes with a share of 39 % to the total bare engine mass. The mass shares for different components are visualized in figure 9. Schmitz et al. predicted a lower increase in total engine mass for WET of $\approx$ 40 % [4]. However, the concept for condensation and water recovery for WET has changed compared to Schmitz et al.

The presented numbers only give a first indication: The bare engine mass for the WET concept is higher compared to the reference system but no show stoppers are found. Due to the larger nacelle length, additional mass penalties have to be expected for WET with respect to the installed power plant mass. It is emphasized that there is still a large uncertainty in the assumptions made and several components are neglected in the mass breakdown structure. Additionally, not all options to further reduce engine mass are explored for the WET concept.

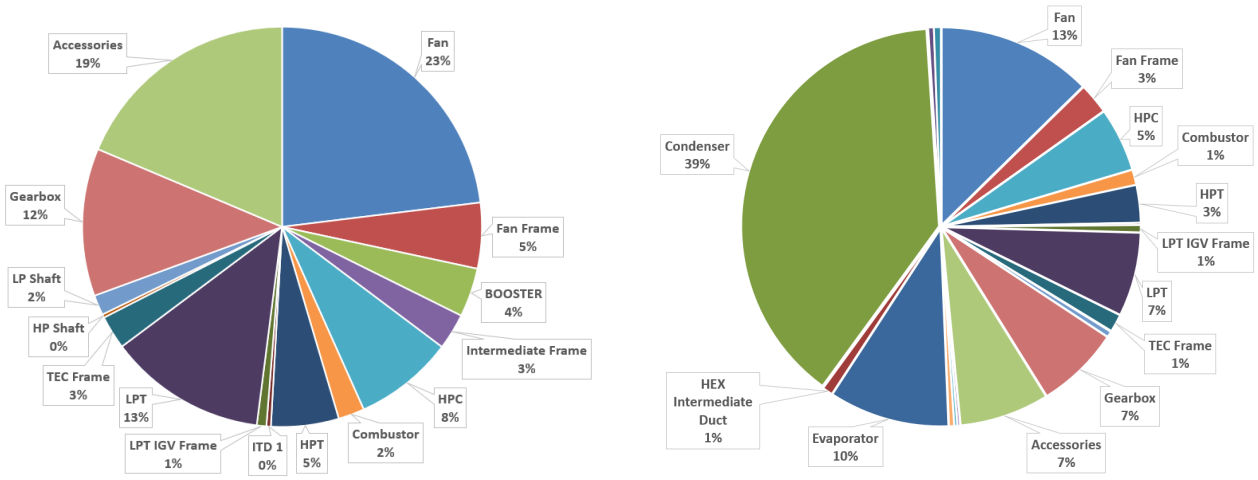

(a) GTF (b) WET

Figure 9 – Comparison of the mass shares for the WET concept and a conventional geared turbofan.

4. Parameter Studies

In this section, design variations of the BPR and OPR are presented for the WET concept and resulting trends in engine mass and dimensions are discussed. The used thermodynamic model is presented in part A of this work [12]. All designs are obtained by applying the workflow presented in section 2.5 and fulfill the same set of requirements with respect to flight conditions, thrust capability and off-takes. When one of the parameters BPR, OPR or T_4 is varied, the other parameters remain unchanged. Further design parameters of the WET concept are also kept constant: share of the bypass air that flows through the condenser, pressure at which the water is provided to the evaporator, expansion ratio of the steam turbine, speed ratio of the nozzles, minimum temperature difference for the evaporator.

4.1 Bypass Ratio

Figure 10a shows the trends for the thrust specific fuel consumption (TSFC), engine length, engine mass, fan diameter and mission fuel burn. The parameter 'mission fuel burn' describes how the fuel mass that is burned during a typical mission changes for a variation of the engine design accounting for penalties related to engine efficiency, dimensions and mass (see part A [12]). The other plots in figure 10 are presented to discuss the trends of overall engine parameters. The following observations are made:

- With increasing BPR, the specific thrust of the engine decreases. This leads to an increase in propulsive efficiency and continuously reduces the TSFC. In order to provide the required thrust capability, the mass flow through the engine's inlet and the fan diameter grow.
- With an increasing bypass ratio, the core flow exits the turbine section with a lower exhaust gas temperature T_5 (see figure 10c). The lower gas temperature diminishes the extractable amount of energy that can be used to provide superheated steam. Therefore, the water-to-air ratio (WAR) at which the WET is operated shrinks with increasing BPR and less heat has to be transferred by the heat exchangers (see figure 10b).
- When the WET uses a lower water-to-air ratio, the exhaust gas temperature at the condenser inlet is higher. However, an almost constant temperature at the condenser outlet has to be reached to ensure that the water loss to the ambience equals the amount of water that is produced during combustion. Therefore, the reduction in the transferred heat with increasing BPR is smaller for the condenser as for the evaporator (see figure 10b).
- The logarithmic temperature differences for the condenser strongly increase with BPR: higher temperature difference between the inlet and outlet of the exhaust gas as well as lower temperature of the bypass air at the outlet since less heat is transferred to the bypass flow. As a result, the length of the condenser decreases significantly for higher $BPRs$ (10d).
- The length of the evaporator slightly increases with BPR. This is related to the assumption of a fixed Mach number at the evaporator inlet. Due to a lower temperature and speed of sound at the inlet, the resulting inflow velocity decreases and a larger frontal area is required for growing $BPRs$.
- The increase in turbo engine length is mainly driven by a larger fan at higher $BPRs$.
- For $BPR \leq 20$, the condenser length dominates the trend of the total engine length and with increasing BPR the total length decreases. For $BPR \geq 20$, the evaporator drives the total length, which leads to the reversal of the trend for the total engine length in figure 10a. The minimum length is achieved for BPR = 22.
- The mass of the heat exchanger assembly decreases for higher $BPRs$. Only the intermediate duct gains mass for BPR > 20 since the axial distance that has to be bridged between the heat exchangers grows. At BPR = 20, the outlets of the evaporater and condenser have a similar axial position and the duct mass reaches a minimum. The mass of the turbomachinery

assembly is mainly driven by the growing fan dimensions and mass at higher $BPRs$. As a result of the counteracting trends for the turbomachinery assembly and heat exchanger assembly, the total bare engine mass has a minimum at $BPR > 28$ (see Fig. 10a).

- The mission fuel burn also reaches a minimum for $BPR > 28$. However, the trend of the mission fuel burn is rather flat and the selection of a lower BPR between 24 to 28 with lower length seems to be reasonable (see Fig. 10a).

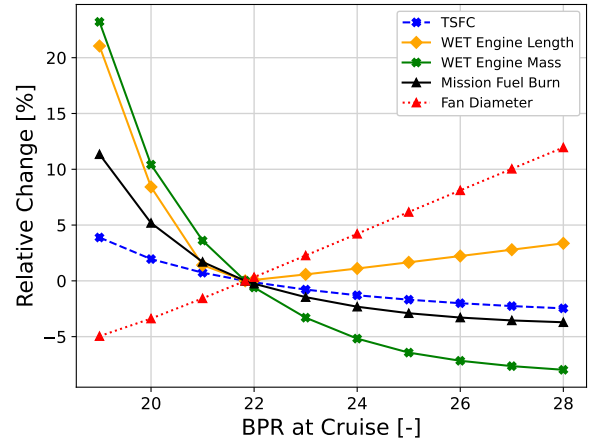

(a) Overall Parameters

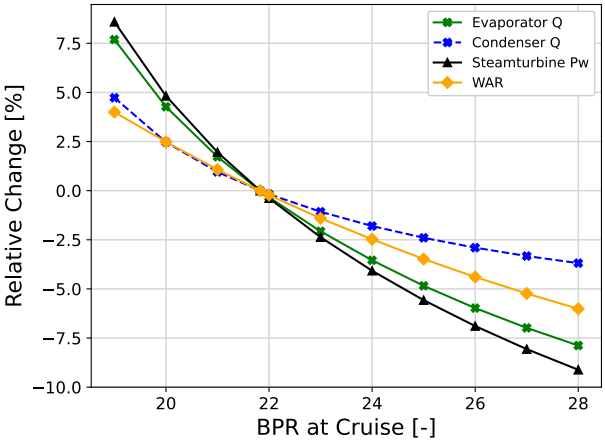

(b) Water Circuit Parameters

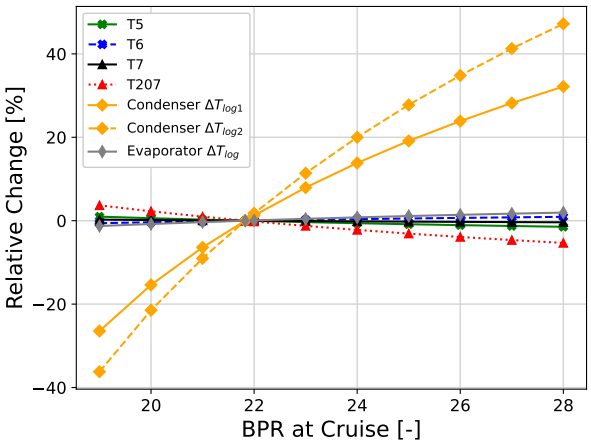

(c) Cycle Temperatures

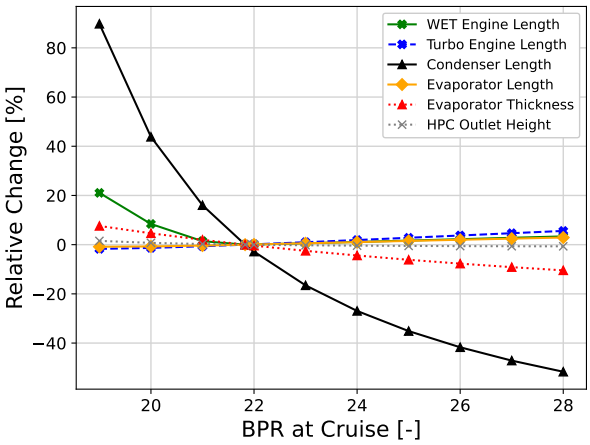

(d) Dimensions

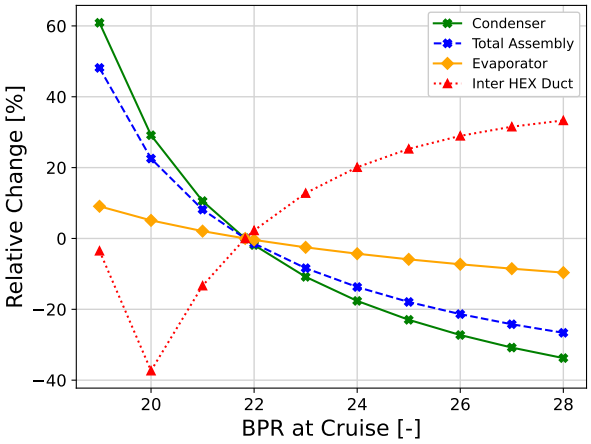

(e) Mass Heat Exchanger Assembly

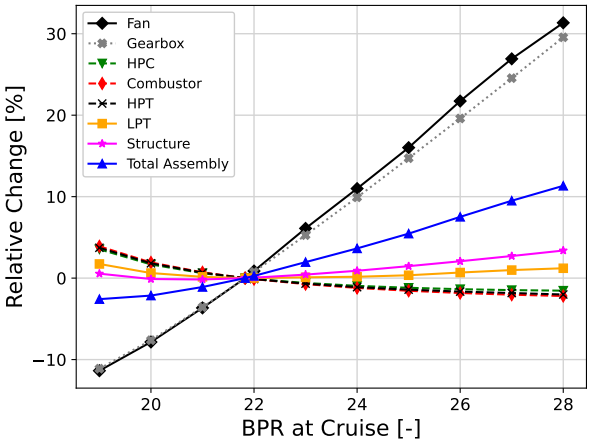

(f) Mass Turbomachinery Assembly

Figure 10 – Resulting trends for a variation of the bypass ratio BPR.

4.2 Overall Pressure Ratio

Figure 11a shows the trends for the thrust specific fuel consumption (TSFC), engine length, engine mass, fan diameter and mission fuel burn. The other plots in figure 11 are presented to discuss the trends of these overall engine parameters. The following observations are made:

- A higher OPR and therefore, a higher pressure level of the Joule-Brayton cycle results in an improvement of TSFC but also in less specific power provided by the core: Maintaining the combustor outlet temperature T_4 leads to a lower fuel-to-air ratio (FAR) at higher pressure levels. In consequence, the mass flow through the engine has to be increased with OPR to provide the required thrust. This leads to a continuously growing mass flow and fan diameter.

- With an increasing OPR, the core flow exits the turbine section with a lower exhaust gas temperature T_5 (see figure 11c). The lower gas temperature diminishes the extractable amount of energy that can be used to provide superheated steam. Therefore, the water-to-air ratio (WAR) at which the WET is operated is lowered with increasing OPR and less heat has to be transferred by the evaporator (see figure 11b). This effect is similar to the trend presented for the BPR even if the change in WAR is much higher for the investigated range of OPR.

- In contrast, the heat that has to be transferred by the condenser almost remains the same (see figure 11b): The inlet temperature at the condenser increases with OPR and an almost constant temperature at the condenser outlet has to be reached to ensure that the water loss to the ambience equals the amount of water that is produced during combustion. Additionally, the core mass flow, which has to be cooled down, grows with OPR. These effects counteract the impact of a lower water content in the exhaust flow and the corresponding lower latent heat that is required to condense the water.

- The logarithmic temperature differences for both the evaporator and condenser strongly increase with OPR due to the already discussed temperature levels (see figure 11c). In combination with less transferred heat for the evaporator, the thickness of the evaporator and the length of the condenser decrease with growing OPR (10d). The length of the evaporator increases with OPR since the core mass flow grows and a constant radial inflow Mach number is assumed. For $OPR \leq 28$, the condenser length drives the total engine length.

- With respect to turbomachinery size and mass, there are two counteracting effects: With increasing OPR and core mass flow, the component size increase. However, due to the higher pressure level in the intermediate region of the core engine, the size of high-pressure components shrinks.

- In terms of the turbomachinery length, an elevated pressure level and the effect of an increased mass flow almost cancel each other over the investigated range of OPR: A higher OPR leads to a smaller combustor and HPT but longer low-pressure components. An additional stage of the HPC is required for $OPR \geq 34$ which elevates the level of the core engine length by 4 %. This discrete step in length due to the additional stage is also reflected a dominate change in the total engine length at high $OPRs$ (see Fig. 11a).

- The mass of the Heat exchanger assembly follows the trend of heat exchanger size and falls with increasing OPR (see Fig. 11e). Since the length of the condenser changes significantly but the length of the evaporator does not, the axial gap that is bridged by the intermediate duct and therefore, its mass increase with OPR. The increase in length due to the additional HPC stage is also reflected in the mass of the intermediate duct.

- In terms of the mass of individual components of the turbomachinery assembly, different trends are observed (see Fig. 11f). The mass for the combustor and the HPT decreases since a higher pressure leads to smaller dimensions and outweighs the effect of additional core mass flow. The mass for the HPC and LPT increase with OPR. The pressure levels at the inlet of the HPC and outlet of the LPT are almost not affected by the OPR and a higher core mass flow

leads to larger flow areas, annulus radii and dimensions in these regions. The smaller size for the remaining stages (outlet of HPC and inlet of LPT) do not compensate the increase in mass.

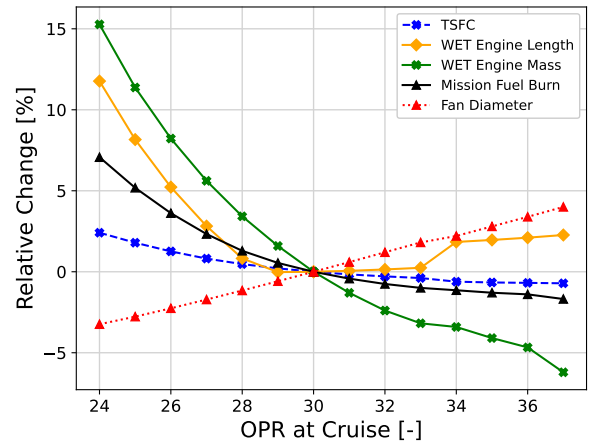

(a) Overall Parameters

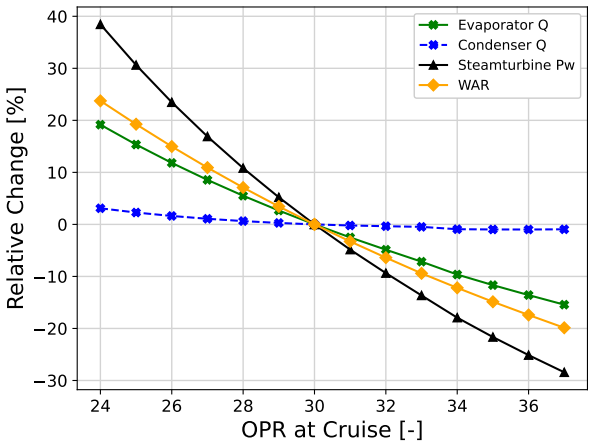

(b) Water Circuit Parameters

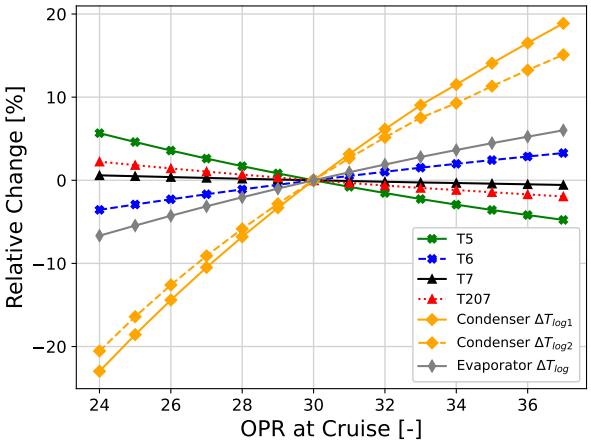

(c) Cycle Temperatures

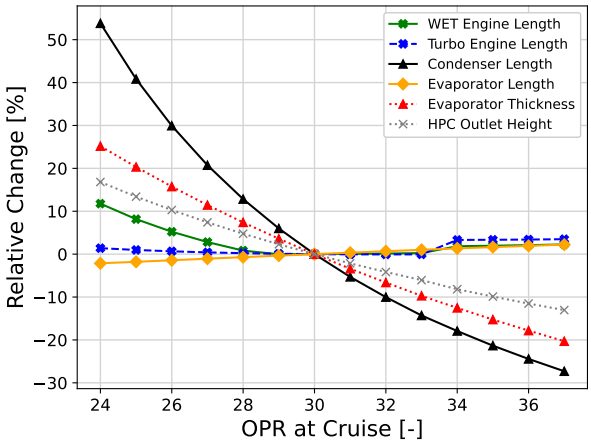

(d) Dimensions

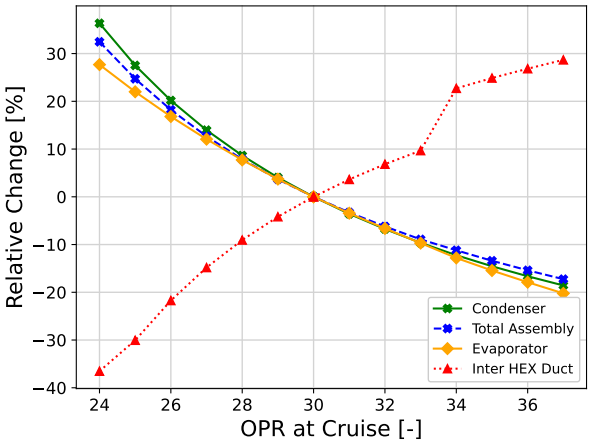

(e) Mass Heat Exchanger Assembly

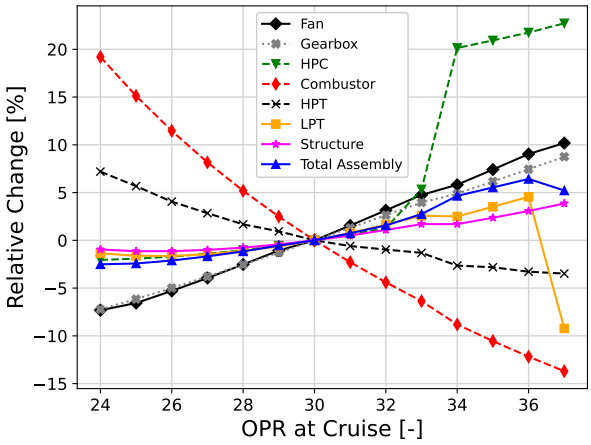

(f) Mass Turbomachinery Assembly

Figure 11 – Resulting trends for a variation of the overall pressure ratio OPR.

- The trend for the HPC has two discrete steps that are related to a change in material and stage number. With increasing OPR and stage pressure ratio, there are higher temperatures after each compressor stage. From $OPR = 32$ to $OPR = 33$, the required material for an intermediate

stage switches from Titan to Nickel-based alloy leading to a higher density and mass (see Fig. 11f). For $OPR \geq 34$, an additional stage is required to be in line with the stage loading limit and there is another discrete step in HPC mass. The discrete step in LPT mass for $OPR > 36$, is also related to a change in material: Here, the temperature at the last stage of the LPT is low enough to use Titanium-Aluminid for the rotor blade and the corresponding disk becomes lighter.

- The mass of the turbomachinery assembly increases and the mass of the heat exchanger assembly decreases with rising OPR. Overall, the trend for the total bare engine mass presented in figure 11a constantly falls with OPR.
- The trend of the parameter mission fuel burn is rather flat, especially for $OPR > 30$. All designs with $OPR > 30$ fall below the minimum required blade height of 10.5 mm at the last HPC stage. Therefore, the highest feasible OPR is 30.

5. Model Limitations

The following model limitations are emphasized:

- The applied models for heat exchanger sizing are based on simple equations using an overall logarithmic temperature difference and assuming a constant overall heat transfer coefficient. The results of the evaporator model are verified for one design by comparison with a higher-fidelity tool using the same boundary conditions. For the condenser no verification was done due to the lack of appropriate models and therefore, a higher uncertainty has to be expected.
- The size of heat exchangers is selected for cruise conditions but other operating conditions may be sizing. Especially, the condenser size strongly depends on the target value for the water recovery rate at sea level operation, during climb or at hot day operation with $\Delta T_{ISA} > 0$.
- The geometrical design space of the heat exchangers is not explored. Selecting other values for the tube diameter, wall thickness, spacings or fins may have the potential to improve heat transfer and to reduce size and mass. Especially, the engine length could be reduced allowing higher inflow velocities and pressure losses for the evaporator.
- Several components that are required to operate the WET concept are not modeled in terms of system mass: Water recovery unit, steam turbine, distribution piping for the recirculating water, actuators and valves. However, these missing positions in the mass breakdown structure are expected to have a rather small share compared to the heat exchangers.
- The Mach number at the inlet of the condenser is too high in order to achieve an acceptable pressure loss for the bypass air that flows through the condenser. This work assumes that an adequate integration concept with moderate pressure loss is implemented. However, this integration concept probably needs higher frontal areas at the condenser inlet which is not reflected yet. In consequence, the condenser length and channel height may be underestimated.

6. Conclusion

In order to investigate the overall dimensions and mass for the WET concept, models for flow path and mass prediction are extended by WET specific components. These conceptual design models are combined with a thermodynamic model of the WET concept and are integrated into a multidisciplinary workflow to investigate the WET design space. Compared to a next generation geared turbofan with the same diameter, an increase of 36 % in engine length and 84 % in total bare engine mass is predicted for the WET concept. These moderate values indicate that the WET concept could be feasible and encourage further more detailed investigations. Additionally, the trend of dimensions and mass are discussed for variations of the bypass ratio and the overall pressure ratio: The overall pressure ratio is limited to moderate values ≤ 30 by the blade height of the last compressor stage. The optimal bypass ratio in terms of mission fuel burn is found to be close to 28. Future research activities should focus on the integration of higher-fidelity models for the heat exchangers into overall system analysis. Additionally, the development and assessment of concepts for integrating the condenser into the

bypass channel avoiding high levels of pressure loss or integration space are of major importance. Furthermore, models for currently missing positions in the mass breakdown structure are required.

7. Copyright Statement

8. Acknowledgments

The research work associated with this publication has been supported by the German Federal Ministry for Economic Affairs and Climate Action under grant number 20M2110B. The funding of the work through the 2nd call of the Federal Aviation Research Program VI (LuFo VI-2), grant project title 'DINA2030plus', is gratefully acknowledged. The authors would like to thank MTU Aero Engines for the close cooperation in the project and the discussions on the Water-Enhanced Turbofan concept.

Supported by:

on the basis of a decision
by the German Bundestag

References

[1] European Commission. Fly the green deal: Europe's vision for sustainable aviation. 2022.

[2] Daniel Silberhorn, Katrin Dahlmann, Alexander Görtz, Florian Linke, Jan Zanger, Bastian Rauch, Torsten Methling, Corina Janzer, and Johannes Hartmann. Climate impact reduction potentials of synthetic kerosene and green hydrogen powered mid-range aircraft concepts. *Applied Sciences*, 12(12):5950, 2022.

[3] Arne Seitz, Markus Nickl, Florian Troeltsch, and Kathrin Ebner. Initial assessment of a fuel cell—gas turbine hybrid propulsion concept. *Aerospace*, 9(2):68, 2022.

[4] Oliver Schmitz, Hermann Klingels, and Petra Kufner. Aero engine concepts beyond 2030: Part 1—the steam injecting and recovering aero engine. *Journal of Engineering for Gas Turbines and Power*, 143(2), 2021.

[5] Oliver Schmitz, Sascha Kaiser, Hermann Klingels, Petra Kufner, Martin Obermüller, Martin Henke, Jan Zanger, Felix Grimm, Simon Schuldt, Anna Marcellan, Daniele Cirigliano, Peter Kutne, Alex Heron-Himmel, Stephan Schneider, Judith Richter, Bernhard Weigand, Anne Göhler-Stroh, Arne Seitz, and Mirko Hornung. Aero engine concepts beyond 2030: Part 3—experimental demonstration of technological feasibility. *Journal of Engineering for Gas Turbines and Power*, 143(2), 2021.

[6] Dah Yu Cheng and Albert L. C. Nelson. The chronological development of the cheng cycle steam injected gas turbine during the past 25 years: Gt-2002-30119. *Journal of Engineering for Gas Turbines and Power*, pages 421–428, 2002.

[7] Dah Yu Cheng. The distinction between the cheng and stig cycles. In *Proceedings of the ASME Turbo Expo 2006*, pages 101–116, New York, NY, 2006. ASME.

[8] Sascha Kaiser, Oliver Schmitz, Paul Ziegler, and Hermann Klingels. The water-enhanced turbofan as enabler for climate-neutral aviation. *Applied Sciences*, 12(23):12431, 2022.

[9] Richard Becker, Florian Wolters, Mobin Nauroz, and Tom Otten. Development of a gas turbine performance code and its application to preliminary engine design. *Deutscher Luft- und Raumfahrtkongress DLRK*, 2011.

[10] Stanislaus Reitenbach, Maximilian Vieweg, Richard Becker, Carsten Hollmann, Florian Wolters, Jens Schmeink, Tom Otten, and Martin Siggel. Collaborative aircraft engine preliminary design using a virtual engine platform, part a: Architecture and methodology. In *AIAA Scitech 2020 Forum*, 2020.

[11] Stanislaus Reitenbach, Jens Schmeink, Marius Bröcker, Marvin Nöthen, and Martin Siggel. GTlab — a C++ framework for collaborative engineering. `https://github.com/dlr-gtlab/`, 2023.

[12] Alexander Görtz, Jannik Häßy, Markus Nickl, Alexandros Lessis, Marc Schmelcher, and Mahmoud El-Soueidan. On the water enhanced turbofan concept: Part a - thermodynamics and overall engine design. *ICAS*, 2024.

[13] Jannik Häßy and Jens Schmeink. Knowledge-based conceptual design methods for geometry and mass estimation of rubber aero engines. *ICAS*, 2022.

[14] Hubert Grieb, editor. *Projektierung von Turboflugtriebwerken*. Technik der Turboflugtriebwerke. Birkhäuser Basel, Basel and s.l., 2004.

[15] Marc Schmelcher, Jannik Häßy, Alexander Görtz, and Mahmoud El-Soueidan. Methods for the preliminary design of heat exchangers in aircraft engines. In *Proceedings of ASME Turbo Expo 2023: Turbomachinery Technical Conference and Exposition (GT 2023)*, New York, N.Y., 2023. the American Society of Mechanical Engineers.

[16] Stefan Bretschneider. *Knowledge-Based Preliminary Design of Aero-Engine Gas-Generators*. Dissertation, Universität Stuttgart, Stuttgart, 2011.

[17] Jannik Häßy, Martin Bolemant, and Richard-Gregor Becker. An educated guess - predicting turbomachinery efficiencies of aero engines during conceptual design. In *Proceedings of ASME Turbo Expo 2023: Turbomachinery Technical Conference and Exposition (GT 2023)*, New York, N.Y., 2023. the American Society of Mechanical Engineers.